World Academy of Science, Engineering and Technology
International Journal of Mechanical and Mechatronics Engineering
Vol:12, No:6, 2018

Pull-In Instability Determination of Microcapacitive Sensor for Measuring Special Range of Pressure

Yashar Haghighatfar, Shahrzad Mirhosseini

Open Science Index, Mechanical and Mechatronics Engineering Vol:12, No:6, 2018 publications.waset.org/10009170.pdf

***Abstract*—**Pull-in instability is a nonlinear and crucial effect that is important for the design of microelectromechanical system devices. In this paper, the appropriate electrostatic voltage range is determined by measuring fluid flow pressure via micro pressure sensor based microbeam. The microbeam deflection contains two parts, the static and perturbation deflection of static. The second order equation regarding the equivalent stiffness, mass and damping matrices based on Galerkin method is introduced to predict pull-in instability due to the external voltage. Also the reduced order method is used for solving the second order nonlinear equation of motion. Furthermore, in the present study, the micro capacitive pressure sensor is designed for measuring special fluid flow pressure range. The results show that the measurable pressure range can be optimized, regarding damping field and external voltage.

***Keywords*—**MEMS, pull-in instability, electrostatically actuated microbeam, reduced order method.

I. Introduction

MICROELECTROMECHANICAL system (MEMS) devices have been widely used in extensive aerospace applications, information technology, and biomaterials. The small size, light weight, and low cost production have been the reason which makes commercialization attractive. These devices are an integration of actuators, mechanical elements, sensors, and electronics [1], [2]. Microbeams have been extensively used in MEMS applications over past decades. Indeed, simple configuration, low energy consumption and appropriate compatibility of electrically actuated microbeam devices have attracted researchers'attentions. The actuated microbeam model consists of an elastic beam suspended over a ground plate, and dielecteric fills the gap between them [3]. While the voltage exceeds a critical point, the elastic beam deflects and collapses. This phenomenon is a crucial point in MEMS designing and known as pull-in instability [4], [5], [7]. The static displacement and stress of clamped – clamped beam under various loadings based on shooting model was investigated by Choi and Lovel [6]. They promoted size dependent microbeam model for predicting the pull-in. Zhang and Zhao [5] have introduced a numerical and analytical method for studying pull-in instability of microstructures under electrostatic force. They developed a one-mode approach based on Galerkin reduced order method gathering with Cardan's solution of cubic equation. Recently, the utilization of microbeams coupled with fluid flow in MEMS devices has been reported for measuring pressure. In this case, the investigators show their interest in micro-fluid devices such as micropump, biomedical, and biological MEMS applications [8]-[10]. Puers and Baert [11] performed voltage analysis of electrostatically actuated beam structures with fixed–fixed and fixed–free end conditions. They presented closed form solution for the pull-in voltage based on lumped spring–mass system. Sadeghian [12] examined the application of the generalized differential quadrature method to the study of pull-in. Ho and Tai [13] opened up a new territory for flow control with MEMS. Although, there are many researches working on dynamics of microbeams containing internal flow without electrostatic field, the dynamic and pull-in instability of microbeam conveying fluid flow is limited. In this article, a theoretical model is applied to predict dynamic and pull-in instability for measuring fluid pressure. In the proposed model, the influence of nonlinear electrostatic force [14], microstructure and damping field is considered in MEMS devices to optimize the design for measuring special ranges of harmonic pressure.

Yashar Haghighatfar is with the Mechanical Engineering, AmirKabir University of Technology, Tehran, Iran (corresponding author, e-mail: y.haghighatfar@aut.ac.ir).

Shahrzad Mirhosseini is with the Mechanical Engineering, AmirKabir University of Technology, Tehran, Iran.

II. Materials and Methods

The governing equations using Euler-Bernoulli beam theory with damping effects, are written as follows

$$EI\frac{\partial^4 y_{(x,t)}}{\partial^4 x}+\rho s\frac{\partial^2 y_{(x,t)}}{\partial^2 t}+c\frac{\partial y_{(x,t)}}{\partial t}=f_{(x,t)} \tag{1}$$

Based on Galerkin method, beam equation is discretized in order to compute equivalent stiffness, mass and damping

$$y_{(x,t)}=\sum_{i=1}^{n}\psi_i(x).\varphi_i(t) \tag{2}$$

in which the shape function satisfies boundary conditions and determines the time participation coefficient of each mode shape. Substituting (2) in (1) leads to

$$EI\frac{\partial^4\sum_{i=1}^{n}\psi_i(x).\phi_i(t)}{\partial x^4}+\rho s\frac{\partial^2\sum_{i=1}^{n}\psi_i(x).\phi_i(t)}{\partial t^2}+c\frac{\partial\sum_{i=1}^{n}\psi_i(x).\phi_i(t)}{\partial t}=\mathrm{Re} \tag{3}$$

Open Science Index, Mechanical and Mechatronics Engineering Vol:12, No:6, 2018 publications.waset.org/10009170.pdf

In (3), Re indicates the residual of equation, and ρ, s are density and transverse cross section, respectively. According to Galerkin method, the obtained residual must be orthogonal with shape functions resulting in

$$\int_0^l \psi_j(x).\mathrm{Re}.\mathrm{dx} = 0 \tag{4}$$

Substituting (3) in (1) leads to

$$\begin{aligned}&\sum_{i=1}^{n} EI\varphi_i(t)\int_0^l \psi_i(x)^{IV}\psi_j(x).\mathrm{dx}+\\&\sum_{i=1}^{n} \rho s\ddot{\varphi}_i(t)\int_0^l \psi_i(x)\psi_j(x).\mathrm{dx}+\\&\sum_{i=1}^{n} C\dot{\varphi}_i(t)\int_0^l \psi_i(x)\psi_j(x).\mathrm{dx} = 0\end{aligned} \tag{5}$$

Introducing the equivalent stiffness, mass and damping matrices as follows

$$\sum_{i=1}^{n} EI\int_0^l \psi_i(x)^{IV}\psi_j(x).\mathrm{dx} = k_{ii} \tag{6}$$

$$\sum_{i=1}^{n} \rho s\int_0^l \psi_i(x)\psi_j(x).\mathrm{dx} = m_{ii} \tag{7}$$

$$\sum_{i=1}^{n} C\int_0^l \psi_i(x)\psi_j(x).\mathrm{dx} = c_{ii} \tag{8}$$

Governing equation of motion is discretized as below

$$m_{ii}\ddot{\varphi}_i(t) + c_{ii}\dot{\varphi}_i(t) + k_{ii}\varphi_i(t) = 0 \tag{9}$$

In order to speculate the most accurate shape function, damping coefficient is eliminated in (9) and the remained equation is solved as

$$\begin{aligned}&y_i(x) = a\sin(\lambda_i(x)) + b\sin(\lambda_i(x)) +\\&\alpha_i(c\cos(\lambda_i(x)) + d\cosh(\lambda_i(x)))\end{aligned} \tag{10}$$

Substituting (10) into (9) and inserting the boundary condition for cantilevered micro-beam, the shape function's coefficients are

$$a = 1, b = -1, c = -1, d = 1, a_i = \frac{\sin(\lambda_i x) + \sinh(\lambda_i x)}{\cos(\lambda_i x) + \cosh(\lambda_i x)}$$

By solving the characteristic equation, the modes shape is derived as the following relations

$$\begin{aligned}&\cos\lambda_i(l).\cosh\lambda_i(l) = -1\\&\lambda_1(l) = 1.875\\&\lambda_2(l) = 4.6941\end{aligned} \tag{11}$$

By inserting the first mode shape and the coefficients into (10), the shape function for the cantilevered beam is

$$\begin{aligned}&y_i(x) = \sin(\lambda_1(l)) - \sinh(\lambda_1(l)) +\\&\frac{\sin\lambda_1(l) + \sinh\lambda_1(l)}{\cos\lambda_1(l) + \cosh\lambda_1(l)}(-\cos(\lambda_1(l)) - \cosh(\lambda_1(l)))\end{aligned} \tag{12}$$

The equivalent stiffness, damping, and mass matrix is attained by inserting (12) in (6) and (7) and solved with Maple software. As a result, the natural frequency of the system can be introduced as below, where $k_{ii} = 3.5$, $w_{ii} = 2.39\times10^5$.

$$w_{ii} = \sqrt[2]{\frac{k_{ii}}{m_{ii}}} \tag{13}$$

A. Static and Dynamic Analysis of Pull-In Phenomenon

According to static (14) and considering the spring force, the equilibrium equation between spring and elecrostatic force can be introduced as

$$F_e + F_s = F_e - kx_d = 0 \tag{14}$$

On the other hand, the electrostatic force is derived according to (14). The electrostatic force, based on voltage, is introduced as

$$F_e = \frac{\xi A V_{ext}^{\ 2}}{2.(x_0 - x_d)^2} \tag{15}$$

Inserting (15) into (14), the voltage is achieved based on other parameters and variables.

$$V_{ext} = \sqrt{\frac{2kx_d(x_0 - x_d)^2}{\xi A}} \tag{16}$$

The static pull-in can happen while the external voltage reaches the maximum value. The appropriate static voltage is determined as before by some assumptions. In reality, the micropressure sensor has the acceleration and works in a viscous area. In this case, the governing equation is defined

$$m_{ii}\ddot{x}(t) + c_{ii}\,\dot{x}(t) + kx(t) = \frac{\xi_0 A V_{ext}^{\ 2}}{2.(x_0 - x_d)^2} \tag{17}$$

B. Reduced order Model

Nonlinear (17) can be solved numerically. In this case, the Runge-Kutta method is used to reach precise results. The

Open Science Index, Mechanical and Mechatronics Engineering Vol:12, No:6, 2018 publications.waset.org/10009170.pdf

introduced second order differential equation is changed to two separate first order differential equations in state space as:

$$y_1(t) = x(t)$$

$$y_2(t) = \dot{x}(t)$$

$$\dot{y_1}(t) = y_2(t) \tag{18}$$

$$\dot{y_2}(t) = -\frac{k}{m}.y_1(t) - \frac{c}{m}y_2(t) + \frac{\xi A v_{ext}^{\ 2}}{2m(x-x_0)^2}$$

TABLE I
THE GEOMETRICAL AND MATERIAL PROPERTIES OF THE STUDIED MODEL

Symbol	L	b	h	d	ρ
Property	Length	Width	Height	Initial gap	Density
Value	250	50	3	1	2332
Unit	µm	µm	µm	µm	kg/m^3

III. RESULT AND DISCUSSION

In this article, the static and dynamic pull-in analysis of Euler-Bernoulli micro cantilevered beam is investigated. The physical, geometrical, and mechanical parameters of Euler-Bernoulli microbeam are considered in Table I.

a. Pull-in instability analysis of Euler-Bernoulli microbeam

In this part, the effect of voltage ranges, distinct damping coefficient and frequency of the sensor's pressure ranges are discussed. Firstly, the static voltage range is determined by solving (16) numerically. Although, the dynamic pull-in in pressure sensor occurs in a real case, the static pull-in voltage range is the key point of design at the beginning.

Fig. 1 depicts the static pull-in voltage range due to the gap (x=1 µm), where the static pull-in value is equal to v=14.2663. The result shows that the sensor fails for the voltage values over v=14.2663 and the appropriate voltage range should be considered lower than this value.

The effect of different damping coefficients for cantilevered microbeam in electrostatic field is shown in Fig. 2, and comparison between three damping coefficients, $c = 0$, $c = 0.2c_{cr}$, c_{cr}, is depicted in this figure. Although the dynamic pull-in voltage is increased in all three types, the maximum range happens where $c = c_{cr}$. So, it is revealed that increasing damping coefficient postpones dynamic pull-in, and the voltage ranges are increased. It is noted that, with decreasing the external voltage, the initial deflection of Euler Bernoulli microbeam decreases, that this point leads to enhanced measurable pressure sensor range.

According to Fig. 3, the sensor pressure range is increased in damping field. Compared with Figs. 3 (a) and (b), the measurable pressure range is extended where damping coefficient is high. It is clear that the pressure range is enhanced significantly due to $c = c_{cr}$, $v = 1$. In this case, the measurable pressure sensor range is up to 5065 Pa.

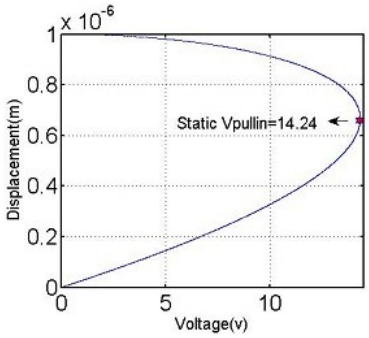

Fig. 1 Stability region with external voltage for a microbeam

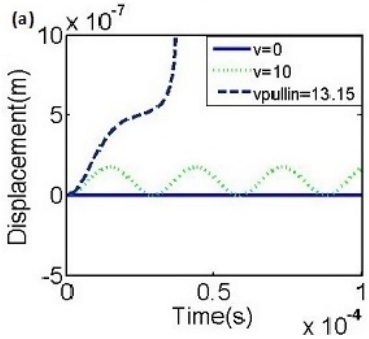

Fig. 2 (a) Pull-in voltage stability region in non-damping field(c=0)

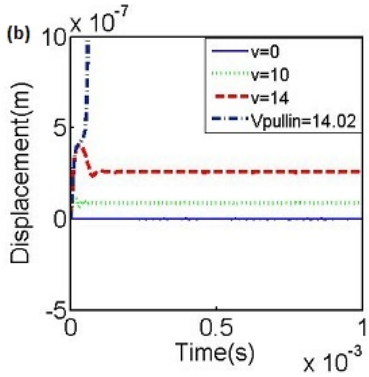

Fig. 2 (b) Pull-in voltage Stability region in damping field (c=0.2 ccr)

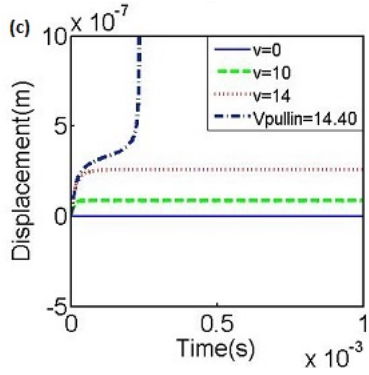

Fig. 2 (c) Pull-in voltage Stability region in damping field (c= ccr)

Open Science Index, Mechanical and Mechatronics Engineering Vol:12, No:6, 2018 publications.waset.org/10009170.pdf

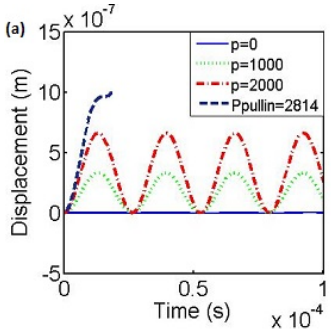

Fig. 3 (a) Pull-in pressure Stability region in non damping field(c=0)

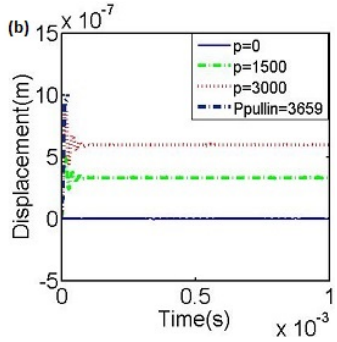

Fig. 3 (b) Pull-in pressure Stability region in damping field (c=0.2ccr)

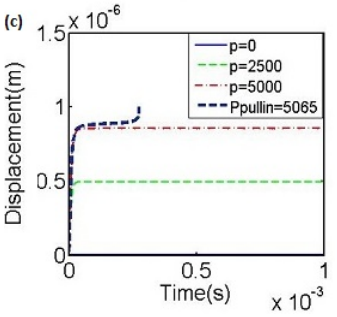

Fig. 3 (c) Pull-in voltage Stability region in damping field (c=ccr)

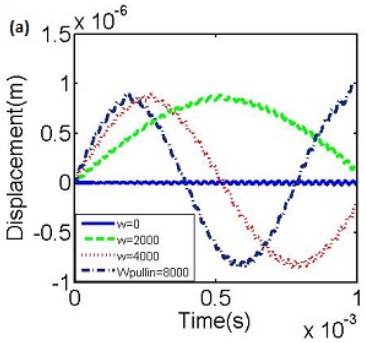

Fig. 4 (a) Measurable Frequency range in non-damping field (c=0)

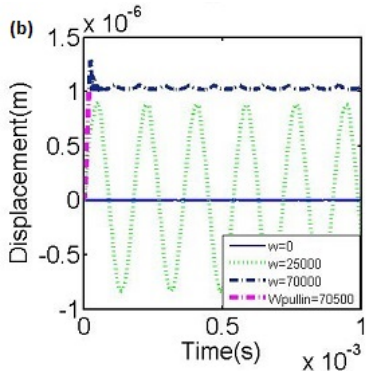

Fig. 4 (b) Measurable frequency range in damping field (c=0.2ccr)

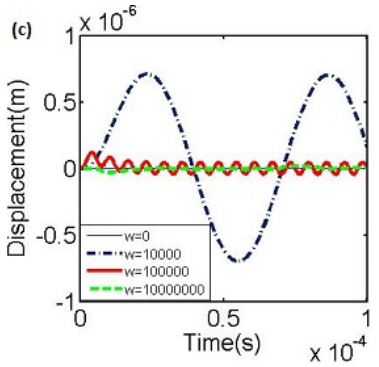

Fig. 4 (c) Measurable frequency range in damping field(c=ccr)

Fig. 4 illustrates the positive influence of damping field on the sensor pressure range. It is noted that, in the reality, pressure which is applied to sensor is not constant. In this case, the pressure is determined by the equation $p = 5000\sin(\omega t)$. Fig. 4 (a) shows that, for the pressure value, $p = 5000(pa)$, $c = 0$, $v = 1$, the frequency range is restricted and the sensor fails in the frequency value of $\omega = 8000$. According to Figs. 4 (b) and (c) the frequency range is increased in damping field. Regarding to Fig. 4 (c), it should be mentioned that when $c = c_{cr}$, the extent range of frequency can be measured. So, the dynamic pull-in is not probable.

Fig. 5 shows that the capacity of designed micro pressure sensor increases significantly in damping field. Comparing Fig. 5 (c) with Figs. 5 (a) and (b), the dynamic pull-in time is the lowest. The sensor capacity is also higher than the two other ones. It is stated that the dynamic pull-in occurs exactly at the pressure that was mentioned in Fig. 3.

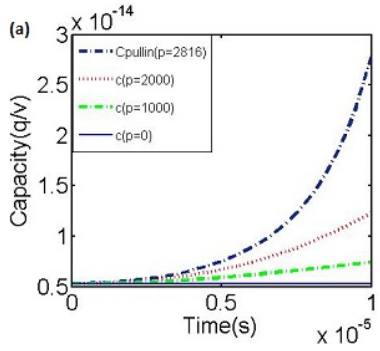

Fig. 5 (a) Capacity of designed micro pressure sensor in non-damping- field (c=0)

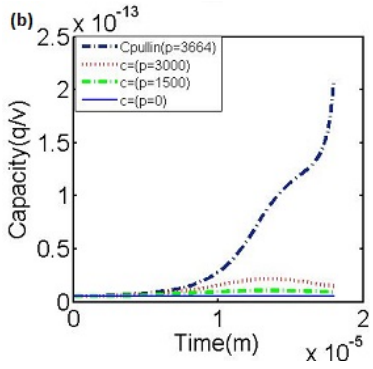

Fig. 5 (b) Capacity of designed micro pressure sensor in damping-field (c=0.2ccr)

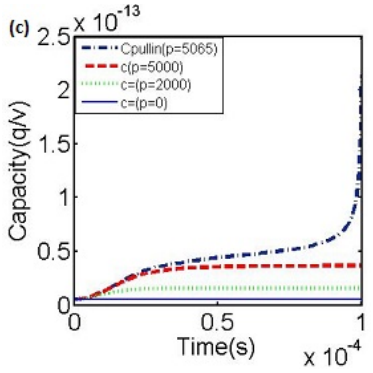

Fig. 5 (c) Capacity of designed micro pressure sensor in damping - field (c=ccr)

IV. Conclusion

In this paper, the static and dynamic pull-in of Euler-Bernoulli micro cantilevered beam based on Galerkin method under elec- trostatic field, using Runge-Kutta second order approach is studied. In this study, the dimensions of pressure sensor are in microscale. The effect of distinct damping fields on measurable pressure ranges is also illustrated. Furthermore, the sensor is de- signed for measuring a wide range of frequency with the highest measurable pressure range. The result of this paper can be listed as below.

1) The static pull-in voltage occurs in value of $v = 14.24$. The external voltage should be applied at the values lower than $v < 14.24$ to prevent static pull-in phenomenon
2) The dynamic pull-in voltage range can be extended in damping field. So, with considering the lower external voltage in that field, the measurable pressure range is developed.
3) At the specified value of damping, the highest measurable pressure value is achieved.
4) The extent range of frequency of harmonic pressure can be measured in damping field. Also the pressure sensor can work in a variety of different frequency values with damping coefficient of $c = c_{cr}$. In addition, the highest pressure value can be measured in this case.

References

[1] Micromachined jets for manipulation of macro flows. Cleveland Heights, OH: Transd. Res. Found. Dussan EB, Davis SH; 1994.
[2] DJ TMC. Glezer A.1994. Micromachined jets for manip- ulation of macro flows. Cleveland Heights, OH: Transd. Res. Found. Dussan EB, Davis SH.
[3] KE E. Dynamic micromechanics on Si: techniques and devices. IEEE Trans Electron Devices. 1978; 25:1241–50.
[4] Nagel DJ. and Zaghloul ME 2001 MEMS: micro technol- ogy, mega impact. IEEE Circuits Devices; 17:14–25.
[5] Electromechanical model of RF MEMS switches. Mi- crosystem Technologies.2003;9(6–7):420–426.
[6] Choi B, Lovell EG .1997. Improved analysis of mi- crobeams under mechanical and electrostatic loads. J Mi- cromech Microeng. 0; 7:24–29.
[7] L .2011a. Size effect on the static behaviour of electrostat- ically actuated microbeams. Acta Mech Sin; 27:445–451.
[8] Chang TP .2013. Nonlinear thermal–mechanical vibra- tion of flowconveying double-walled carbon nanotubes; 0. Subjected to random.
[9] Mattia GY. Review: static and dynamic behavior of liquids inside carbon nanotubes. Microfluid Nanofluid.5:289–305.
[10] Aser DJ, Santiago JG .2004. A review of micropumps. J Micromech Microeng. 0; 14:35–64.
[11] Pull-in voltage analysis of electrostatically actuated beam structures with fixed–fixed and fixed–free end conditions.Pamidighantam S, Puers R, Baert K, Tilmans HAC. 2002; 12:458–464.
[12] Sadeghian H, Rezazadeh G, Osterberg PM .2007. Ap- plication of the generalized differential quadrature method to the study of pull-in. phenomena of MEMS switches. J Microelectromech Syst; 16:1334–1340.
[13] CM TYH. 1996.MEMS and its applications for flow con- trol.J Fluids Eng.
[14] Dumitru I. Caruntu, Israel Martinez.2014. Reduced order model of parametric resonance of electrostatically actuated MEMS cantilever resonators. Journal of Non-Linear Mechanics, 66, 28–32.

Open Science Index, Mechanical and Mechatronics Engineering Vol:12, No:6, 2018 publications.waset.org/10009170.pdf